The geometry of time-optimal trajectories for an omni-directional robot

Paritosh A. Kavathekar and **Devin J. Balkcom**
Department of Computer Science
Dartmouth College
{paritosh, devin}@cs.dartmouth.edu

Matthew T. Mason
The Robotics Institute
Carnegie Mellon University
matt.mason@cs.dartmouth.edu

Introduction

The optimal trajectories are known analytically for only a few ground vehicles: steered cars (Dubins 1957; Reeds & Shepp 1990), and wheel-chair-like differential-drive vehicles (Balkcom & Mason 2002). This paper presents the analytical time-optimal trajectories for a kinematic model of a vehicle of a new class, shown in figure 1(a). The wheels are *omniwheels*; unlike regular wheels, omniwheels slip freely in the direction perpendicular to the controlled direction. The arrangement of wheels allows this robot to drive in any direction without the need to turn first, and to spin as it does so. We model the vehicle as a rigid body in the unobstructed plane, with configuration $(x, y, \theta) \in \mathbf{SE}^2$. We assume that the controls are the angular velocities of the wheels in the powered directions, (v_1, v_2, v_3), and assume that the controls are independently bounded: $v_{\{1,2,3\}} \in [-1, 1]$.

Although the vehicle can move in arbitrary directions in the configuration space, some directions are faster than others. The optimal trajectories consist of sequences of three types of constant controls: spins in place (all three wheels spin at maximum speed in the same direction), arcs of circles, (all wheels spin at maximum speed, but not all in the same direction), and straight lines (two wheels spin at maximum speed in opposite directions, and the third does not spin). We assign a symbol to each constant control: P, C, S, respectively.

No optimal trajectory contains more than 18 control switches, and only certain sequences are ever optimal. There are four classes of optimal trajectory, which we call *spin*, *roll*, *shuffe*, and *tangent*; figure 3 shows an example of each class. This classification is *complete* in the sense that every optimal trajectory must be one of these types, and *minimal* in the sense that for each class there exists a pair of configurations for which *only* a trajectory of that class is optimal.

One focus of QR research is reasoning about continuous systems with some known structure. Optimal trajectories are a fundamental characteristic of a system. Robots expend resources to achieve goals; the simplest resource is time, and the simplest goal is for the system to reach a desired configuration. The time-optimal trajectories are therefore a basic property of the mechanism, and are a basis for complex reasoning about mechanism design, planning among obstacles, or vehicle control. The trajectories also provide a natural metric on the configuration space that is independent of the particular planner or controller applied to the robot; this metric serves as a basis to compare the suitability of planners, controllers, or mechanisms over a particular distribution of tasks.

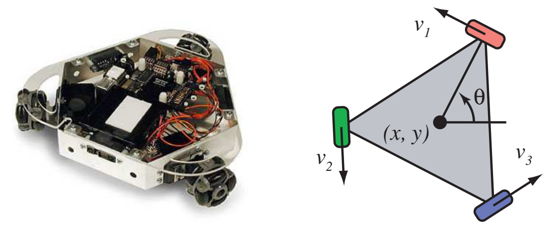

(a) Photograph. (b) Notation.

Figure 1: The Palm-Pilot Robot Kit, an example of an omni-directional vehicle. Photograph used by permission of Acroname, Inc., `www.acroname.com`.

A second focus of QR research is determining geometric characteristics of complex systems. As will be discussed, the optimal trajectories for the robot considered can be described in an very geometric way. All optimal trajectories are from one of four basic classes of trajectories; each class is a family of related curves. Every optimal trajectory can be described by a simple control law on the wheel velocities; the wheel velocities are determined by the location of the vehicle with respect to some a line in the plane.

We do not argue that the 'optimal' trajectories we derive should be used to control a robot. Resources other than time, such as energy, safety, and precision, are also important in choosing good trajectories and following them. Tradeoffs must be made, but understanding the relative payoffs of each choice requires an understanding of the fundamental qualitative behavior of the mechanism. The knowledge that great circles are geodesics on the sphere does not require that airplanes must strictly follow great circles, but may nonetheless influence the choice of flight paths.

Related work

The optimal trajectories, and the mapping between trajectories and pairs of start and goal configurations, have been found for kinematic models of steered cars that can only move forwards (Dubins 1957) and cars that can go forwards or backwards (Reeds & Shepp 1990; Sussmann &

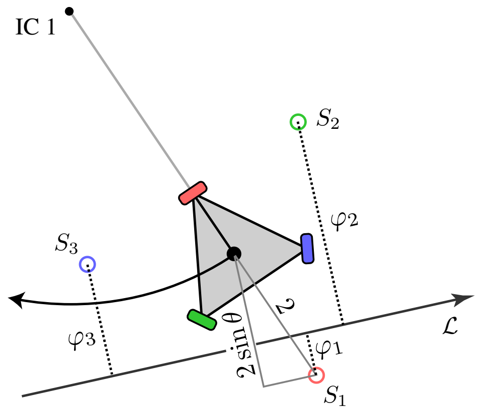

Figure 2: Geometric interpretation of the switching functions. For the case shown, $\varphi_1 < 0$, $\varphi_2 > 0$, and $\varphi_3 > 0$, so the controls are $v_1 = 1$, $v_2 = -1$, and $v_3 = -1$.

Tang 1991; Souères & Boissonnat 1998; Souères & Laumond 1996). Recently, optimal trajectories have been studied in the presence of obstacles (Desaulniers 1996; Vendittelli, Laumond, & Nissoux 1999), for vehicles that are not steered cars, including the differential-drive (Balkcom & Mason 2002), hovercraft (Coombs 2000), and underwater vehicles (Chyba & Haberkorn 2005), and metrics other than time (Chitsaz *et al.* 2006). Determining the optimal controls for dynamic models is difficult, and results include numerical techniques and geometric characterizations (Reister & Pin 1994; Renaud & Fourquet 1997; Kalmár-Nagy, D'Andrea, & Ganguly 2004).

Main results

In this section, we highlight a few of the primary theorems that describe the optimal trajectories. Our primary tool is Pontryagin's Maximum Principle (Pontryagin *et al.* 1962). The Maximum Principle states that there exists an adjoint vector, defined in terms of differential equations in the state and controls, such that the optimal controls must be chosen to minimize the Hamiltonian H, which is the dot product of the adjoint vector and $\dot{q}$, the time derivative of the state. Our model is simple enough that the differential equations describing the adjoint vector may be integrated analytically. Choosing the controls to minimize the Hamiltonian gives the following result:

Theorem 1 *For any time-optimal trajectory of the omni-directional vehicle, there exist constants k_1, k_2, and k_3, with $k_1^2 + k_2^2 + k_3^2 \neq 0$, such that at almost every time t, the value of the control v_i is determined by the sign of the switching function φ_i:*

$$v_i = \begin{cases} 1 & \text{if } \varphi_i < 0 \\ -1 & \text{if } \varphi_i > 0. \end{cases}$$

The switching functions φ_1, φ_2, and φ_3 are given by

$$\varphi_i = 2(-k_1 \sin\theta_i + k_2 \cos\theta_i) + (k_1 y - k_2 x + k_3),$$

where θ_i is the angle the line from the center to wheel i makes with the x-axis. Furthermore, the quantity λ_0 defined by

$$\lambda_0 = -H(\varphi_1, \varphi_2, \varphi_3) = |\varphi_1| + |\varphi_2| + |\varphi_3|$$

is constant along the trajectory.

The functions φ_i are known as *switching functions* because the corresponding control switches when φ_i changes sign. In the generic case, none of the switching functions are zero, so all of the controls are either 1 or -1: the robot spins in place or follows a circular arc. If a switching function is zero, the optimal control must be determined by other means. Although we omit the details, it turns out that in this *singular* case, the only control which may be optimal is translation along a line connecting the center of the robot and a wheel.

Satisfaction of the Maximum Principle is a necessary, but not sufficient, condition for trajectories to be optimal. We will say that any trajectory that satisfies the Maximum Principle is *extremal*. The results presented in the following sections depend on a detailed local analysis of the switching functions, use of the local properties given in theorem 1 to determine the global structure of the extremal trajectories, and analysis of the geometry of extremal trajectories to derive further necessary conditions on optimal trajectories.

The Maximum Principle does not give direct information about the number of control switches in an optimal trajectory. We have shown that extremal trajectories are well-behaved: there are only a finite number of switches in an extremal trajectory; the number is upper-bounded by a constant that depends only on λ_0.

The Maximum Principle also gives no direct information about the constants of integration k_1, k_2, and k_3, as these depend on the initial and final configurations of the robot. In this paper, we give the structure of trajectories as a function of these constants, but do not describe how to determine the constants.

Geometric interpretation of the switching functions

Theorem 1 may be stated in a more geometric form.

Theorem 2 *Define the points S_1, S_2, and S_3 rigidly attached to the vehicle, with distance 2 from the center of the vehicle, and making angles of $180°$, $300°$, and $60°$ with the ray from the center of the vehicle to wheel 1, respectively (refer to figure 2). For any time-optimal trajectory, there exist constants k_1, k_2, and k_3, and a line (the switching line)*

$$\mathcal{L} = \{(a, b) \in \mathbf{R}^2 : k_1 b - k_2 a + k_3 = 0\},$$

such that the controls of the vehicle v_1, v_2, and v_3 depend on the location of the points S_1, S_2, and S_3 relative to the line. Specifically, for $i \in \{1, 2, 3\}$,

$$v_i = \begin{cases} 1 & \text{if } S_i \text{ is to the right of the switching line,} \\ -1 & \text{if } S_i \text{ is to the left of the switching line.} \end{cases}$$

The switching functions are invariant to translation of the vehicle parallel to the switching line (see figure 2), and scaling the switching functions by a positive constant does not affect the controls. Therefore, for any optimal trajectory, we may without loss of generality choose a coordinate frame with x-axis on the switching line, and an appropriate scaling, such

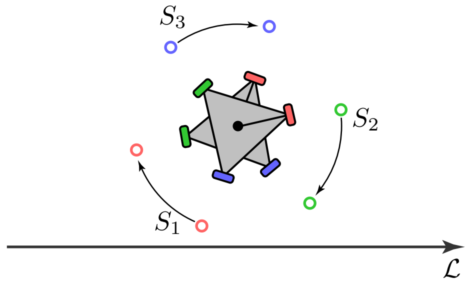

(a) An example clockwise **spin** trajectory, P_-.

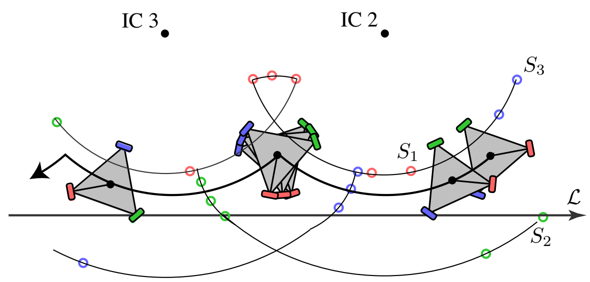

(b) A **rollCW** trajectory, $\mathrm{C}_{2-}\mathrm{P}_-\mathrm{C}_{3-}\mathrm{P}_-\mathrm{C}_{1-}$.

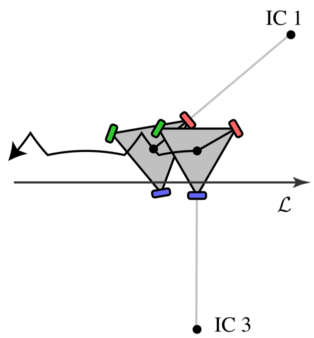

(c) A **shuffle**: $\mathrm{C}_{3+}\mathrm{C}_{1-}\mathrm{P}_-\mathrm{C}_{2-}\mathrm{C}_{3+}\mathrm{C}_{1-}\mathrm{P}_-$.

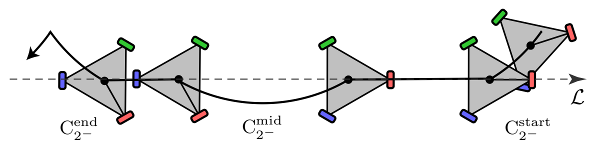

(d) A **tangent** trajectory, $\mathrm{C}_{2-}\mathrm{S}_{2,3}\mathrm{C}_{2-}\mathrm{S}_{2,1}\mathrm{C}_{2-}\mathrm{P}_-\mathrm{C}^{\mathrm{start}}_{3-}$.

Figure 3: The four classes of optimal trajectories for an omni-directional robot.

that y gives the distance from the switching line, and θ gives the angle of the vehicle relative to the switching line. With this choice of coordinates, the switching functions become

$$\varphi_i = y - 2\sin\theta_i. \tag{1}$$

Classification of extremal trajectories

Theorem 1 can be used to completely enumerate the optimal controls, and the possible transitions between optimal controls. In this paper, we present only the geometric interpretation of the optimal trajectories given by theorem 2. If we consider all possible initial configurations of the vehicle relative to the switching line, we can see geometrically that there are five cases:

- **SpinCW** and **SpinCCW**. If the vehicle is far from the switching line, then the switching points are on the same side of the switching line and never cross it; the vehicle spins in place indefinitely. An example is shown in figure 3(a). We expect some trajectory of this class to be optimal when the start and goal configurations are at the same (x, y) location.
- **RollCW** and **RollCCW**. If the switching points either straddle the switching line, or the vehicle is close enough to the switching line that spinning in place will eventually cause the switching points to straddle the line, the trajectory is a sequence of circular arcs and spins in place. If the vehicle is far enough from the switching line that every switching point crosses the switching line and returns to the same side before the next switching point crosses the line, the structure of the trajectory is as shown in figure 3(b). We expect some trajectory of this class to be optimal when two configurations are nearby in the workspace, but separated by a significant angular distance.
- **Shuffle**. If the vehicle is close enough to the switching line that two switching points cross the switching line before the first returns to its initial side, the sign of $\dot{\theta}$ changes during the trajectory. An example is shown in figure 3(c). We expect some trajectory of this class to be optimal when the vehicle must move a small distance 'sideways'.
- **Tangent**. As the vehicle spins in place or follows a circular arc, the switching points follow circular arcs. If one of these arcs is tangent to the switching line, a singular control becomes possible at the point of tangency, and the vehicle may translate along the switching line for an arbitrary duration before returning to following a circular arc. We expect some trajectory of this type to be optimal when two configurations are far apart: the robot lines up its fastest translation direction, translates, and corrects orientation with the final circular arcs and spin.
- **Slide**. If two switching points fall on the switching line, the trajectory is doubly singular. The vehicle slides along the switching line in a pure translation. It turns out that although *slide* trajectories are extremal, they are never optimal.

Configuration-space trajectories

The geometric enumeration above is complete. In order to show this, it is useful to consider the structure of trajectories in configuration space. The configuration of the robot relative to the switching line may be represented by (θ, y).

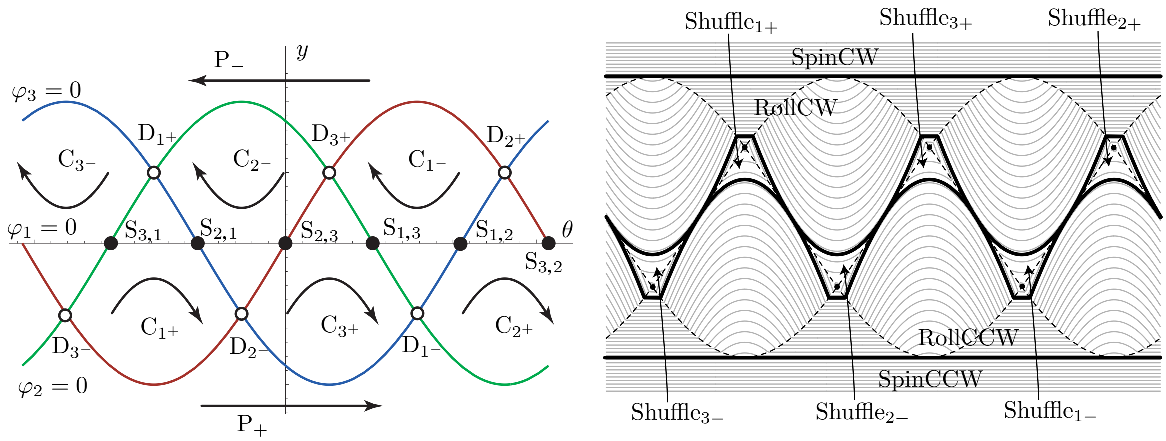

(a) The sinusoidal switching curves partition the configuration space into eight C and P control regions.

(b) Each trajectory corresponds to a level set (contour) of the Hamiltonian. The dashed lines represent control switches; the bold lines separate the trajectory classes.

Figure 4: The configuration space of the robot relative to the switching line.

Each point on figure 4(a) corresponds to a configuration of the robot relative to the switching line. The sinusoidal curves defined by $\varphi_1 = 0$, $\varphi_2 = 0$, and $\varphi_3 = 0$ mark boundaries in configuration space; we call these curves the *switching curves*. The switching curves and their intersections divide the configuration space into cells, within each of which the controls are constant.

The trajectory curves in configuration space can be drawn by considering each possible initial configuration, determining the constant control, and integrating to find the trajectory. When the trajectory crosses a switching curve, the control switches.

The condition that the Hamiltonian remain constant over a trajectory provides an even simpler way to enumerate all trajectories in the configuration space. Each extremal trajectory falls on a level set of the Hamiltonian, and extremal trajectories may be classified by the value λ_0. Figure 4(b) shows the level sets of the Hamiltonian, or equivalently, the image of several extremal trajectories in configuration space.

- If $\lambda_0 > 6$, the level set is a pair of horizontal lines, one with $y = \lambda_0/3$, corresponding to a SpinCW trajectory, and one with $y = -\lambda_0/3$, corresponding to a $\mathrm{SpinCCW}$ trajectory.
- If $2\sqrt{3} \leq \lambda_0 \leq 6$, the level set is composed of two disjoint curves, one corresponding to RollCW trajectory and one corresponding to a $\mathrm{RollCCW}$ trajectory.
- If $\lambda_0 = 2\sqrt{3}$, the level set is the union of the bold curves shown in figure 4(b). $\mathrm{Tangent}$ trajectories follow these curves.
- If $3 < \lambda_0 < 2\sqrt{3}$, the level set is composed of six disjoint curves, one corresponding to each of the six symmetric $\mathrm{Shuffle}$ trajectories.
- If $\lambda_0 = 3$, the level set is six isolated points, each corresponding to one of the six Slide trajectories.

Optimal trajectories

We have presented the five classes of extremal trajectories; every optimal trajectory must be extremal. However, not all extremal trajectories are optimal. In fact, *slide* trajectories, although extremal, are never optimal, since every *slide* may be replaced by a faster *shuffle*. Furthermore, finite-time extremal trajectories have a maximum number of switches that is upper-bounded by λ_0; a much stronger result can be proven for optimal trajectories, which are subsections of extremal trajectories:

Theorem 3 *Optimal trajectories contain no more than 18 control switches. Specifically,*

(i) optimal spin trajectories contain zero control switches, and the maximum duration of an optimal spin trajectory is π;

(ii) optimal roll trajectories contain at most 8 control switches;

(iii) optimal shuffle trajectories contain at most 7 control switches;

(iv) optimal tangent trajectories contain at most 12 control switches if the trajectory is non-monotonic in θ, and at most 18 control switches if the trajectory is monotonic in θ;

For *roll*, *shuffle*, and *tangent* trajectories, the approach of the proof is to consider a trajectory with more segments than the corresponding bound, and show that by slicing and rearranging the segments, a non-extremal trajectory of equal time can be constructed. Since the constructed trajectory is not extremal, neither it nor the original can be optimal.

Finally, the derived classification of trajectory by λ_0 is minimal:

Theorem 4 *Spin, Roll, Shuffle, and Tangent trajectories are each optimal for at least one pair of start and goal configurations of the omni-directional vehicle.*

Open problems

Although the results described apply only to a particular type of robot, we hope that expanding the number of examples of systems for which the exact time-optimal trajectories are known from three to four is a step towards a better qualitative and quantitative understanding of the relationship between mechanism design and the use of resources. The primary focus of future work is on generalizations; in fact, we have recently shown (in unpublished work) that the optimal trajectories for a large class of wheeled vehicles can be described by constant controls that switch as the vehicle crosses a switching line.

References

Balkcom, D. J., and Mason, M. T. 2002. Time optimal trajectories for differential drive vehicles. *International Journal of Robotics Research* 21(3):199–217.

Chitsaz, H.; LaValle, S. M.; Balkcom, D. J.; and Mason, M. T. 2006. Minimum wheel-rotation paths for differential-drive mobile robots. In *IEEE International Conference on Robotics and Automation*. To appear.

Chyba, M., and Haberkorn, T. 2005. Designing efficient trajectories for underwater vehicles using geometric control theory. In *24rd International Conference on Offshore Mechanics and Artic Engineering*.

Coombs, A. T. 2000. Time-optimal control of two simple mechanical systems with three degrees of freedom and two inputs. Master's thesis, Queen's University.

Desaulniers, G. 1996. On shortest paths for a car-like robot maneuvering around obstacles. *Robotics and Autonomous Systems* 17:139–148.

Dubins, L. E. 1957. On curves of minimal length with a constraint on average curvature and with prescribed initial and terminal positions and tangents. *American Journal of Mathematics* 79:497–516.

Kalmár-Nagy, T.; D'Andrea, R.; and Ganguly, P. 2004. Near-optimal dynamic trajectory generation and control of an omnidirectional vehicle. *Robotics and Autonomous Systems* 46:47–64.

Pontryagin, L. S.; Boltyanskii, V. G.; Gamkrelidze, R. V.; and Mishchenko, E. F. 1962. *The Mathematical Theory of Optimal Processes*. John Wiley.

Reeds, J. A., and Shepp, L. A. 1990. Optimal paths for a car that goes both forwards and backwards. *Pacific Journal of Mathematics* 145(2):367–393.

Reister, D. B., and Pin, F. G. 1994. Time-optimal trajectories for mobile robots with two independently driven wheels. *International Journal of Robotics Research* 13(1):38–54.

Renaud, M., and Fourquet, J.-Y. 1997. Minimum time motion of a mobile robot with two independent acceleration-driven wheels. In *Proceedings of the 1997 IEEE International Conference on Robotics and Automation*, 2608–2613.

Souères, P., and Boissonnat, J.-D. 1998. Optimal trajectories for nonholonomic mobile robots. In Laumond, J.-P., ed., *Robot Motion Planning and Control*. Springer. 93–170.

Souères, P., and Laumond, J.-P. 1996. Shortest paths synthesis for a car-like robot. *IEEE Transactions on Automatic Control* 41(5):672–688.

Sussmann, H., and Tang, G. 1991. Shortest paths for the Reeds-Shepp car: a worked out example of the use of geometric techniques in nonlinear optimal control. SYCON 91-10, Department of Mathematics, Rutgers University, New Brunswick, NJ 08903.

Vendittelli, M.; Laumond, J.; and Nissoux, C. 1999. Obstacle distance for car-like robots. *IEEE Transactions on Robotics and Automation* 15(4):678–691.